Defect and Diffusion Forum
ISSN: 1662-9507, Vol. 434, pp 45-49
doi:10.4028/p-u3d2Yi

Submitted: 2023-10-02
Revised: 2024-04-16
Accepted: 2024-04-16
Online: 2024-08-22

Investigation of Dislocation Behaviors in 4H-SiC Substrate during Post-Growth Thermal Treatment

Hongyu Peng[1,a], Yuhan Gao[1,b], Zhiqiang Shi[1,c], Yani Pan[1,d], Can Zhu[1,e], Chao Gao[1,f*], Balaji Raghothamachar[2,g], Michael Dudley[2,h]

[1]SICC Co., Ltd., No. 99 South TianYue Road, Jinan, 25000, China

[2]Department of Materials Science & Engineering, Stony Brook University, Stony Brook, NY 11794 USA

[a]penghongyu@sicc.cc, [b]gaoyuhan@sicc.cc, [c]shizhiqiang@sicc.cc, [d]panyani@sicc.cc, [e]zhucan@sicc.cc, [f]gaochao@sicc.cc, [g]balaji.raghothamachar@stonybrook.edu, [h]michael.dudley@stonybrook.edu

Keywords: 4H-SiC substrate, Basal Plane Dislocations, Annealing

Abstract. Dislocation behaviors after post-growth thermal treatment were investigated by X-ray topography and KOH etching. Generation of prismatic dislocations were observed in X-ray topography, and density of basal plane dislocations (BPDs) increases with annealing temperature and radial temperature gradient. Distribution of newly generated BPDs in the wafer after thermal treatment is correlated to the resolved shear stress arising from radial temperature gradient.

Introduction

4H-SiC is increasingly used in power devices because of its superior physical properties compared to silicon [1]. However, defects such as dislocations still cannot be fully eliminated even using the state-of-the-art growth techniques and these dislocations could deleteriously influence the performance of devices [2&3]. The behavior of the dislocations during crystal growth process has been well documented [4-6]. Basal plane dislocations (BPDs) usually nucleate at the periphery of the crystal and glide toward inner regions under thermal stresses, they can also generate from stress centers such as inclusions, micropipes and polytype boundaries [7]. Despite most BPDs can be converted to TEDs after epitaxial growth [8], some unconverted BPDs can dissociate into partials and the stacking faults expand as partial dislocations glide [9&10], causing degradation of devices. Therefore, the understanding and control of the formation of BPDs are important.

Behaviors of BPDs under thermal treatment have been intensively investigated. It was reported in both substrates and epitaxial layers that BPDs can be converted to TEDs after high temperature annealing [11&12], and the TED segments in epitaxial layers can glide in [1-100] prismatic plane [11]. It was also observed that BPD half loops could be formed from the surface of the epitaxial wafer after annealing [13], and pre-existing BPD segments in epitaxial layer can glide to form interfacial dislocations [13&14].

In this study, we report the multiplication of BPDs and formation of prismatic dislocations after thermal treatment. BPDs were formed from surface source while prismatic dislocations were formed by the glide of TEDs. The density of BPDs increases with annealing temperature and radial temperature gradient. Distribution of newly generated BPDs in the wafer after thermal treatment is correlated to the resolved shear stress arising from radial temperature gradient.

Experiment

Samples used in this study are 6-inch and 8-inch n-type 4H-SiC crystals and substrates fabricated in SICC Co. Ltd. The crystals were grown by physical vapor transport (PVT) technology with 4° off-cut toward 11-20. These wafers were then annealed at high temperatures. X-ray topography (Rigaku XRTmicron) 11-20 reflection was carried out to characterize prismatic dislocations. Standard KOH etching was applied to study BPDs.

Results and Discussion

Fig. 1 (a) is 11-20 X-ray topograph of an area of a 6-inch wafer before thermal treatment. In this area, those dark linear features are BPDs, while the dark dots are threading mixed dislocations that are slightly inclined to sample surface. No prismatic dislocations were observed before thermal treatment. Fig. 1 (b) is the topograph of the same region after thermal treatment. The most striking features are those dark segments along <11-20> directions. They are prismatic dislocations lying in {1-100} prismatic planes. The absence of micropipes or inclusions in surrounding area suggests that these prismatic dislocations were likely formed by the glide/climb of TEDs under the influence of radial thermal stresses [6].

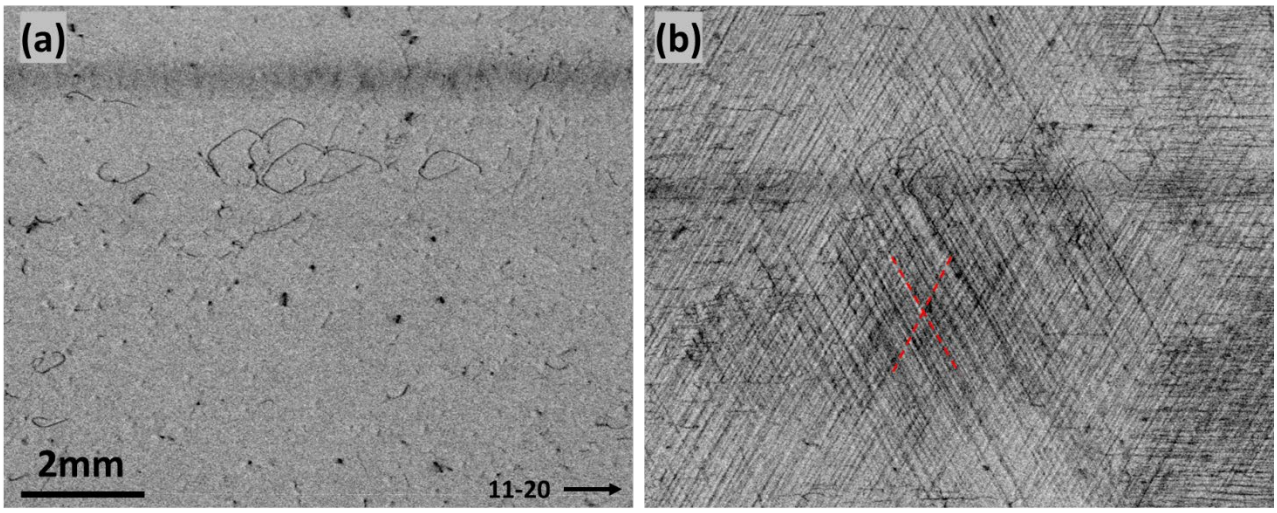

Fig. 1 Rigaku X-ray topography 11-20 reflection of the substrate (a) before thermal treatment and (b) after thermal treatment. Line directions of prismatic dislocations are indicated by the dashed red lines.

In addition to the generation of prismatic dislocations, BPD multiplication is also observed in the wafers after thermal treatment. Fig. 2 (a) is KOH etching image of an 8-inch wafer that was not annealed, showing no BPD slip band. In its sister wafer that was annealed under high temperature, BPD slip bands were generated (Fig. 2 (b)). The slip band is almost symmetrical up and down as its structure is shown in the magnified KOH etching image (Fig. 2 (c)). In the center of the slip band, there are two BPD etch pits pointing towards each other (Fig. 2 (c)). They are the initial state of a BPD half loop generated from sample surface. Under thermal stresses, BPD half loop expands towards the inner region of the wafer and new half loops are generated at the original position. As a result, BPD density dramatically increases after thermal treatment. The mechanism of BPD half loop expansion is schematically illustrated in Fig. 2 (d).

When the wafers were annealed at different conditions, the density of BPDs after annealing would be quite different. Four 8-inch wafers cut from the same boule (these four wafers are close to each other) were annealed at different temperatures. As shown in Fig. 3 (a), BPD density increases from ~1000/cm^2 to ~9000/cm^2 as annealing temperature increases from 1900°C to over 2200°C. Moreover, the density of BPD is not only influenced by annealing temperature, but also temperature gradient. Despite it is well accepted that BPDs arise because of nonlinear axial temperature gradient during crystal growth process of SiC with offcut angles, radial temperature gradient also plays a role in the formation and migration of BPDs since both axial and radial stresses can be resolved onto basal planes. Fig. 3 (b) shows the density of BPD after two different annealing processes (process 1 & 2). Radial temperature gradient in process 2 is bigger than that in process 1. Apparently, at either temperature 1 or 2 (T2>T1), more BPDs were generated when radial temperature gradient is bigger.

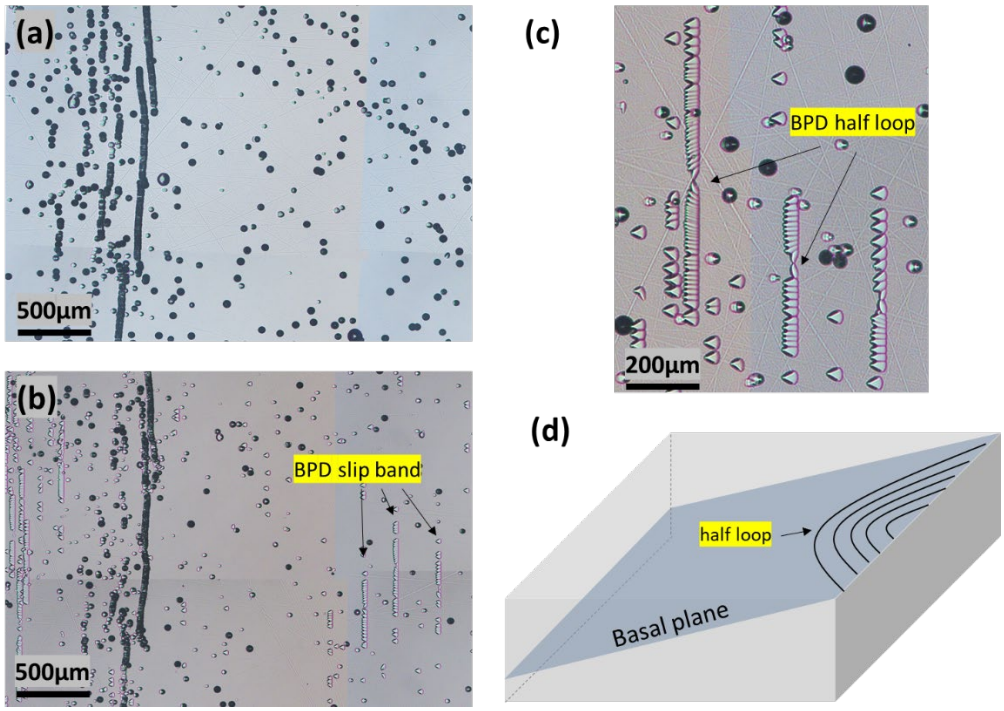

Fig. 2 KOH etching image of two sister wafers that were not annealed (a) and annealed (b). (c) Magnified KOH etching image of dislocation slip band. (d) Schematic illustration of BPD half loop expansion.

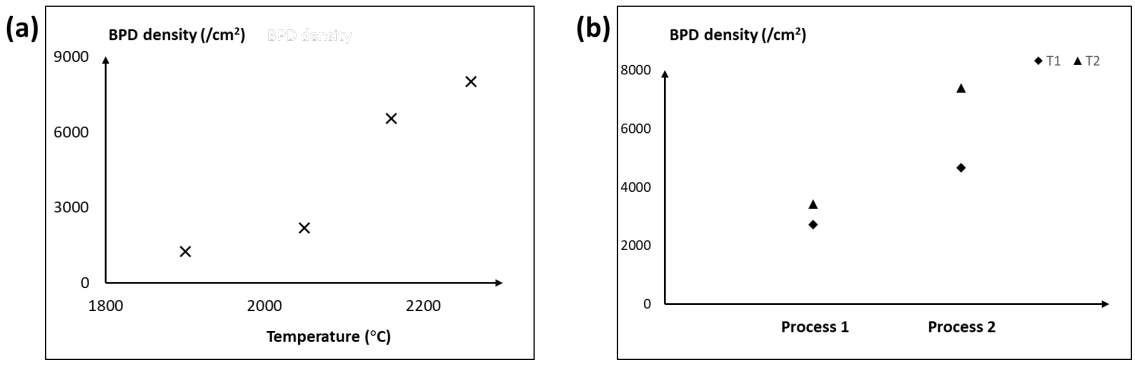

Fig. 3 (a) Plot of BPD density of four wafers from the same boule annealed at different temperatures. (b) BPD density of another four wafers from the same boule after being annealed by processes 1 and 2 (Radial temperature gradient in process 2 is bigger than that in process 1) at temperature 1 and 2 (T2>T1). BPD density was measured by KOH etching.

Generation and multiplication of BPDs during annealing process are thought to be correlated to the resolved shear stress on the basal plane arising from radial temperature gradient. The radial and tangential stress components due to radial temperature gradient is given by [14]:

$$\sigma_{rr} = \alpha E \left[\frac{1}{R^2}\int_0^R T(r) r\, dr - \frac{1}{r^2}\int_0^r T(r) r\, dr\right] \quad (1)$$

$$\sigma_{\theta\theta} = \alpha E \left[\frac{1}{R^2}\int_0^R T(r) r\, dr + \frac{1}{r^2}\int_0^r T(r) r\, dr - T(r)\right] \quad (2)$$

where α is thermal expansion coefficient, E is Young's modulus and R is the radius of the wafer. Expressing the stress components in Cartesian coordinates, only σ_{xx} resolves shear stress on BPD considering its slip direction and the normal of the slip plane:

$$\sigma_{xx} = \sigma_{rr} \cos^2\theta + \sigma_{\theta\theta} \sin^2\theta \quad (3)$$

And the resolved shear stress is:

$$\tau = \sigma_{xx} \cos 4^\circ \sin 4^\circ \quad (4)$$

Fig. 4 (a) is a typical BPD density map of an 8-inch wafer after thermal treatment, where the red/blue color indicates higher/lower BPD density. As shown in the map, BPD density is significantly higher in the central and top/bottom peripheral region of the wafer. During annealing process, the temperature is higher in the periphery while lower in the center (dT/dr>0). Importing temperature profile into Eq. (1) & (2), the calculated relative value of the resolved shear stress is plotted in Fig. 4 (b). It's shown in Fig. 4 (b) that the sign of the stress changes from positive to negative (stress changes from tensile to compressive) from center to top/bottom periphery, indicating that the sign of the Burgers vector of BPDs formed in the periphery and center is opposite. More importantly, the absolute value of resolved shear stress is bigger in the central and top/bottom peripheral regions. The distribution of BPDs after thermal treatment is consistent with the distribution of resolved shear stress, suggesting that the generation and multiplication of BPDs during annealing process is primarily caused by radial temperature gradient.

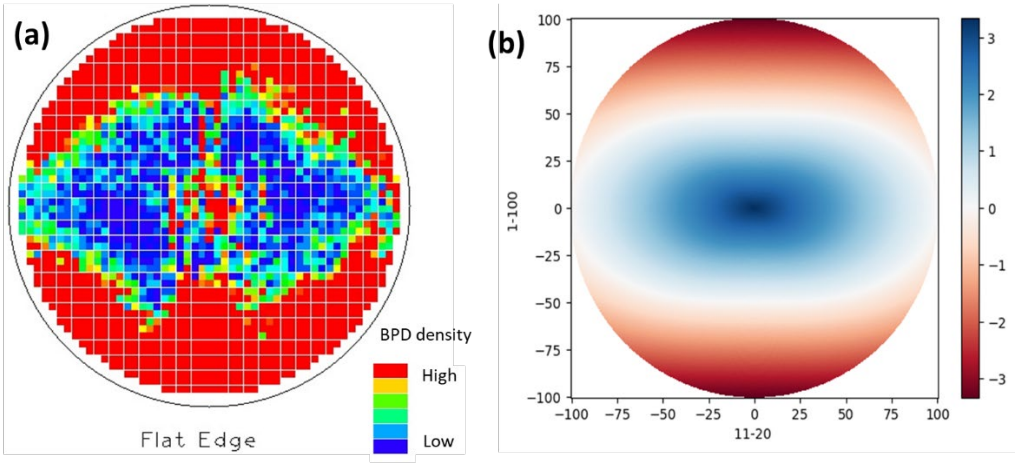

Fig. 4 (a) BPD density map of 8-inch wafer after annealing (evaluated by KOH etching). (b) Plot of the calculated relative value of resolved shear stress from Eq. (3) & (4).

Summary

Different thermal treatments were applied to 4H-SiC substrates. Prismatic dislocations were generated by the glide of TEDs after thermal treatment. BPDs were formed as half loops from the surface and expand into inner regions. The density of BPDs increases with annealing temperature and radial temperature gradient. Distribution of newly generated BPDs in the wafer after thermal treatment is correlated to the resolved shear stress arising from radial temperature gradient.

References

[1] T. Kimoto and J. A. Cooper, Fundamentals of Silicon Carbide Technology, (Wiley IEEE press, Singapore, 2014)

[2] H. Fujiwara, H. Naruoka, M. Konishi, K. Hamada, T. Katsuno, T. Ishikawa, Y. Watanabe and T. Endo, Appl. Phys. Lett. 100, 242102 (2012)

[3] T. Kimoto, A. Iijima, H. Tsuchida, T. Miyazawa, T. Tawara, A. Otsuki, T. Kato and Y. Yonezawa 2017 IEEE International Reliability Physics Symposium pp. 2A-1.1-2A-1.7 (2017)

[4] S. Byrappa, H. Wang, F. Wu, Y. Zhang, B. Raghothamachar, G. Choi, E. K. Sanchez, D. Hansen, R. Drachev, M.J. Loboda and M. Dudley, MRS Online Proceedings Library 1246 202 (2009)

[5] M. Dudley, H. Wang, F. Wu, S. Byrappa, S. Shun, B. Raghothamachar, E. K. Sanchez, G. Chung, D. Hansen, S. G. Mueller, and M. J. Loboda, MRS Online Proceedings Library 1433 65-76 (2012)

[6] J. Guo, Y. Yang, B. Raghothamachar, J. Kim, M. Dudley, G. Chung, E. Sanchez, J. Quast, and I. Manning, J. Electron. Mater. 46 2040-2044 (2017)

[7] M. Dudley, Y. Chen, X. R. Huang and R. Ma, Mater. Sci. Forum 600-603 (2009) pp 261-266

[8] S. Ha, P. Mieszkowski, M. Skowronski, L.B. Rowland, J. Cryst. Growth, 244 (2002) 257-266

[9] S. I. Maximenko and T. S. Sudarshan, J. Appl. Phys. 97, 074501 (2005)

[10] S. Ha, M. Benamara, M. Skowronski and H. Lendenmann, Appl. Phys. Lett., 83 4957 (2003)

[11] X. Zhang and H. Tsuchida, J. Appl. Phys. 111, 123512 (2012)

[12] N. A. Mahadik, R. E. Stahlbush, E. A. Imhoff, M. J. Tadjer, G. E. Ruland, C. A. Affouda, Mater. Sci. Forum, 858 233-236 (2016)

[13] M. Nagano, H. Tsuchida, T. Suzuki, T. Hatakeyama, J. Senzaki, and K. Fukuda, J. Appl. Phys. 108, 013511 (2010)

[14] X. Zhang, M. Nagano and H. Tsuchida, Mater. Sci. Forum, 679-680 306 (2011)